

Pharmacophore generation and atom-based 3D-QSAR of novel 2-(4-methylsulfonylphenyl)pyrimidines as COX-2 inhibitors

Ujashkumar A. Shah · Hemantkumar S. Deokar · Shivajirao S. Kadam · Vithal M. Kulkarni

Received: 27 April 2009 / Accepted: 11 July 2009 / Published online: 11 August 2009
© Springer Science+Business Media B.V. 2009

Abstract Cyclooxygenase-2 (COX-2) inhibitors are widely used for the treatment of pain and inflammatory disorders such as rheumatoid arthritis and osteoarthritis. A series of novel 2-(4-methylsulfonylphenyl)pyrimidine derivatives has been reported as COX-2 inhibitors. In order to understand the structural requirement of these COX-2 inhibitors, a ligand-based pharmacophore and atom-based 3D-QSAR model have been developed. A five-point pharmacophore with four hydrogen bond acceptors (A) and one hydrogen bond donor (D) was obtained. The pharmacophore hypothesis yielded a 3D-QSAR model with good partial least-square (PLS) statistics results. The training set correlation is characterized by PLS factors ($r^2 = 0.642$, $SD = 0.65$, $F = 82.7$, $P = 7.617 \times 10^{-12}$). The test set correlation is characterized by PLS factors ($Q_{ext}^2 = 0.841$, $RMSE = 0.24$, $Pearson-R = 0.91$). A docking study revealed the binding orientations of these inhibitors at active site amino acid residues (Arg513, Val523, Phe518, Ser530, Tyr355, His90) of COX-2 enzyme. The results of ligand-based pharmacophore hypothesis and atom-based 3D-QSAR give detailed structural insights as well as highlights important binding features of novel 2-(4-methylsulfonylphenyl)pyrimidine derivatives as COX-2 inhibitors which can provide guidance for the rational design of novel potent COX-2 inhibitors.

Keywords Pharmacophore · 3D-QSAR · COX-2 inhibitor · Docking

Introduction

Non-steroidal anti-inflammatory drugs (NSAIDs) are widely used for the treatment of pain, fever, and inflammatory diseases such as rheumatoid arthritis and osteoarthritis. Conventional NSAIDs inhibit cyclooxygenase (COX) enzymes which catalyze the formation of prostaglandins (PGs) from arachidonic acid. The discovery of COX-2 isoform in the 1990s led to the development of a new class of NSAIDs known as selective COX-2 inhibitors [1]. COX-2 is induced in response to proinflammatory conditions, while COX-1 is constitutive and responsible for the maintenance of physiological homeostasis, such as gastrointestinal integrity and renal function. Selective inhibition of COX-2 provides a new class of anti-inflammatory agents with significantly reduced side effects such as gastrointestinal ulcer and renal dysfunction. As a consequence, several selective COX-2 inhibitors, such as celecoxib, rofecoxib, valdecoxib and etoricoxib have been developed [2–5]. However, the recent market withdrawal of rofecoxib due to adverse cardiovascular side effects has raised the concern of safety of selective COX-2 inhibitors [6]. Therefore, there is a need to find new selective COX-2 inhibitors with improved safety profile. Nevertheless, the potential therapeutic applications of selective COX-2 inhibitors have been expanded beyond the areas of analgesia and inflammation, as shown by recent studies on COX-2 that have been focused on cancer and neurodegenerative disorders [7–9].

Pharmacophore is an important and unifying concept in rational drug design that embodies the notion that molecules are active at a particular enzyme or receptor because they possess both a number of chemical features that favor the target interaction and a geometry complementary to it [10]. A pharmacophore hypothesis collects common features distributed in three-dimensional space representing groups in a molecule

U. A. Shah · H. S. Deokar · S. S. Kadam · V. M. Kulkarni (✉)
Department of Pharmaceutical Chemistry, Poona College of Pharmacy,
Bharati Vidyapeeth University, Erandwane, Pune 411038, India
e-mail: vivivips5@gmail.com

that participate in important interactions between drug and active site. Pharmacophore model provides a rational hypothetical picture of the primary chemical features responsible for activity. Since the last few years pharmacophore modeling has been one of the important and successful approach for new drug discovery [10–12]. With regard to docking, structure-based drug design efforts have also increased with the growth of X-ray crystallographic information available for the protein targets. Protein–ligand docking is a popular structure-based design technique, and a wide range of algorithms are currently employed in the pharmaceutical sciences and biotechnology areas [13]. In the present study, an atom-based three-dimensional quantitative structure activity relationship (3D-QSAR) is performed with Pharmacophore Alignment and Scoring Engine (PHASE) [14] and docking analysis with Glide [15] for a series of novel 2-(4-methylsulfonylphenyl)pyrimidine derivatives as COX-2 inhibitors. PHASE is a highly flexible system for common pharmacophore identification and assessment, 3D-QSAR model development, and 3D database creation and searching. By employing a novel, tree-based partitioning algorithm, PHASE exhaustively identifies spatial arrangements of functional groups that are common and essential to the biological activity of a set of high affinity ligands. These pharmacophore hypotheses are validated in a number of ways, including their ability to: (i) rationalize the binding affinities of a training set of molecules of varying activity, (ii) successfully predict the affinities of a test set of molecules, and (iii) selectively retrieve known actives from a database of drug-like molecules. In addition, PHASE uniquely offers the ability to distinguish multiple binding modes through a bi-directional clustering approach applied to bit string representations of the ligand/hypothesis space. Glide has been designed to perform as close to an exhaustive search of the positional, orientation, and conformational space available to the ligand as is feasible, while retaining sufficient computational speed to screen large libraries. Glide uses a series of hierarchical filters to search for possible locations of the ligand in the active site region of the receptor. The shape and properties of the receptor are represented on a grid by different sets of fields that provide progressively more accurate scoring of the ligand pose. The objective of the present study is to develop ligand-based pharmacophore hypothesis and to derive atom-based 3D-QSAR model to find features which are responsible for biological activity of novel 2-(4-methylsulfonylphenyl)pyrimidine derivatives as selective COX-2 inhibitors. Further, the binding mode of the active molecule with the active site amino acid residues of COX-2 enzyme was performed by docking using Glide XP. The developed ligand-based pharmacophore hypothesis gives information about important features of these derivatives for COX-2 inhibitory activity and the cubes generated from atom-based 3D-QSAR studies highlight the structural features required for COX-2 inhibition

which can be useful for further design of more potent COX-2 inhibitors.

Experimental

Pharmacophore modeling

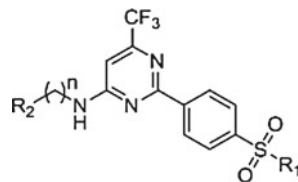
Pharmacophore modeling was carried out using PHASE running on Red Hat Linux WS 3.0 [14, 15]. A set of 63 novel 2-(4-methylsulfonylphenyl)pyrimidine analogs (Tables 1, 2, 3, 4, 5) with available IC_{50} data were taken from literature for the development of ligand-based pharmacophore hypothesis and atom-based 3D-QSAR model [16]. Six compounds were not included in this study due to their high residual value resulting in a better predictive QSAR model.

The negative logarithm of the measured IC_{50} value (pIC_{50}) of whole human blood assay was used in this study. These 63 compounds were divided into a training set (44 compounds) and a test set (19 compounds). The training set molecules were selected in such a way that they contained information in terms of both their structural features and biological activity ranges. The most active molecules, moderately active, and less active molecules were included, to spread out the range of activities [17]. In order to assess the predictive power of the model, a set of 19 compounds was arbitrarily set aside as the test set. The test compounds were selected in such a way that they truly represent the training set.

Generation of common pharmacophore hypothesis

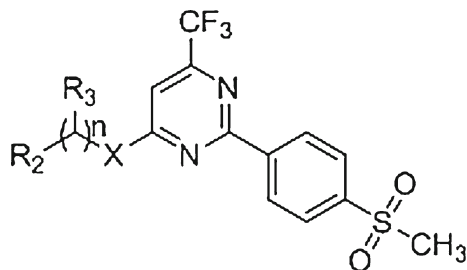
The common pharmacophore hypothesis (CPH) was carried out by PHASE. All molecules were built in Maestro [18]. All ligands were prepared using LigPrep with the OPLS_2005 force field [19]. Conformational space was explored through combination of Monte-Carlo Multiple Minimum (MCM)/Low Mode (LMOD) with maximum number of conformers 1,000 per structure and minimization steps 100 [20, 21]. Each minimized conformer was filtered through a relative energy window of 50 kJ/mol and redundancy check of 2 Å in the heavy atom positions. Common pharmacophoric features were then identified from a set of variants—a set of feature types that define a possible pharmacophore—using a tree-based partitioning algorithm with maximum tree depth of four with the requirement that all actives must match. After applying default feature definitions to each ligand, common pharmacophores containing five and six sites were generated using a terminal box of 1 Å. Scoring of pharmacophore with respect to activity of ligand was conducted using default parameters for site, vector, and volume terms.

These common pharmacophore hypotheses were examined using a scoring function to yield the best alignment of the active ligands using an overall maximum root mean square

Table 1 In vitro COX-2 inhibitory activity of compounds 1–18

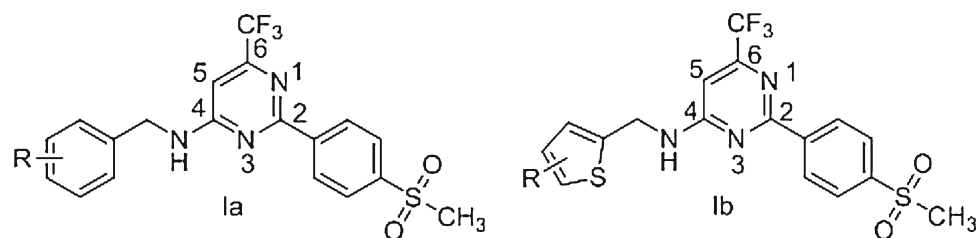
No.	R ¹	R ² (CH ₂) _n	IC ₅₀ (μM)	pIC ₅₀ observed	pIC ₅₀ predicted	No.	R ¹	R ² (CH ₂) _n	IC ₅₀ (μM)	pIC ₅₀ observed	pIC ₅₀ predicted
1	CH ₃		0.071	1.148	0.59	10*	CH ₃		0.083	1.077	0.88
2	NH ₂		0.157	0.802	0.93	11	NH ₂		0.803	0.095	-0.19
3	CH ₃		0.002	2.678	1.77	12	CH ₃		1.48	-0.170	0.21
4	CH ₃		0.046	1.333	0.67	13*	CH ₃		0.789	0.102	0.51
5	NH ₂		3.33	-0.522	-0.15	14	CH ₃		0.028	1.553	0.72
6*	CH ₃		0.298	0.527	0.63	15	CH ₃		0.728	0.138	0.25
7	NH ₂		2.79	-0.446	-0.02	16	CH ₃		0.293	0.533	1.48
8	NH ₂		0.140	0.853	0.83	17	CH ₃		0.238	0.623	0.21
9*	CH ₃		0.14	0.862	0.68	18*	CH ₃		0.475	0.322	0.38

* Compounds used for test set

Table 2 In vitro COX-2 inhibitory activity of compounds 19–23

Compound	X	n	R ₂	R ₃	IC ₅₀ (μM)	pIC ₅₀ observed	pIC ₅₀ predicted
19*	NMe	1	Ph	H	0.454	0.342	0.47
20	S	1	Ph	H	0.527	0.278	0.32
21*	NH	1	Ph	CH ₃	0.521	0.282	0.35
22	NH	2	Thiophen-2-yl	H	1.21	-0.083	0.33
23	NH	2	1-Methyl-1H-pyrrol-2-yl	H	3.98	-0.6	0.17

* Compounds used for test set

Table 3 In vitro COX-2 inhibitory activity of compounds 24–34

Compound	I	R	IC ₅₀ (μM)	pIC ₅₀ observed	pIC ₅₀ predicted
24*	Ia	3,5-diF	0.300	0.522	0.56
25	Ia	4-F	0.077	1.112	0.62
26	Ia	2-CH ₃	5.720	-0.757	0.59
27*	Ia	4-OCH ₃	0.272	0.565	0.53
28	Ia	4-CH ₃	0.048	1.315	0.60
29	Ia	3-CH ₃	1.930	-0.286	0.52
30*	Ia	4-OH	0.635	0.197	0.56
31	Ib	5-CH ₃	0.011	1.932	1.73
32	Ib	3-CH ₃	0.527	0.278	1.51
33*	Ia	4-NH ₂	0.211	0.675	0.56
34	Ib	5-Cl	0.005	2.268	1.75

*Compounds used for test set

deviation (RMSD) value of 1.2 Å with default options for distance tolerance. The quality of alignment was measured by a survival score, defined as:

$$S = W_{\text{site}}S_{\text{site}} + W_{\text{vec}}S_{\text{vec}} + W_{\text{vol}}S_{\text{vol}} \\ + W_{\text{sel}}S_{\text{sel}} + W^m_{\text{rew}}$$

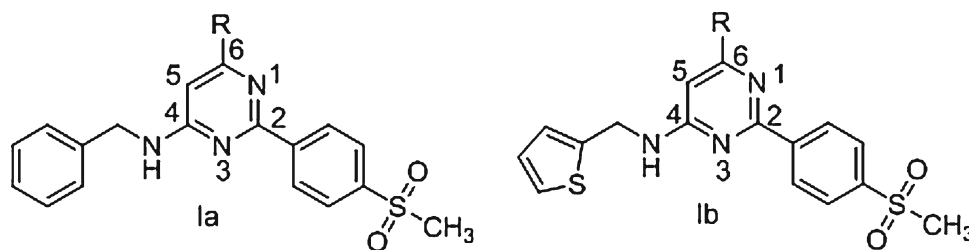
where W are weights and S are scores; S_{site} represents alignment score, the RMSD in the site point position; S_{vec} represents vector score, and averages the cosine of the angles formed by corresponding pairs of vector features in aligned structures; S_{vol} represents volume score based on overlap of van der Waals models of non-hydrogen atoms in each pair of structures; and S_{sel} represents selectivity score, and accounts for what fraction of molecules are likely to match the hypothesis regardless of their activity toward the receptor. W_{site} , W_{vec} , W_{vol} , and W_{rew} have default values of 1.0, while W_{sel} has a default value of 0.0. In hypothesis generation, default values have been used. W^m_{rew} represents reward weights defined by $m - 1$, where m is the number of actives that match the hypothesis.

Pharmacophore-based QSAR do not consider ligand features beyond the pharmacophore model, such as possible steric clashes with the receptor. This requires consideration of the entire molecular structure, therefore an atom-based QSAR model is more useful in explaining the structure–activity relationship. In atom-based QSAR, a molecule is treated as a set of overlapping van der Waals spheres. Each atom (and hence each sphere) is placed into one of six

categories according to a simple set of rules: hydrogens attached to polar atoms are classified as hydrogen bond donors (D); carbons, halogens, and C–H hydrogens are classified as hydrophobic/non-polar (H); atoms with an explicit negative ionic charge are classified as negative ionic (N); atoms with an explicit positive ionic charge are classified as positive ionic (P); non-ionic atoms are classified as electron-withdrawing (W); and all other types of atoms are classified as miscellaneous (X). For purposes of QSAR development, van der Waals models of the aligned training set molecules were placed in a regular grid of cubes, with each cube allotted zero or more ‘bits’ to account for the different types of atoms in the training set that occupy the cube. This representation gives rise to binary-valued occupation patterns that can be used as independent variables to create partial least-squares (PLS) QSAR models. Atom-based QSAR models were generated for all hypotheses using the 44-member training set using a grid spacing of 1.0 Å. The best QSAR model was validated by predicting activities of the 19 test set compounds.

Docking methodology

Docking study was performed on Glide running on Red Hat Linux WS 3.0 [22–24]. The Grid-based Ligand Docking with Energetics (Glide) algorithm approximates a systematic search of positions, orientations and conformations of the ligand in the enzyme-binding pocket via a series of hierarchical filters. The shape and properties of the receptor are

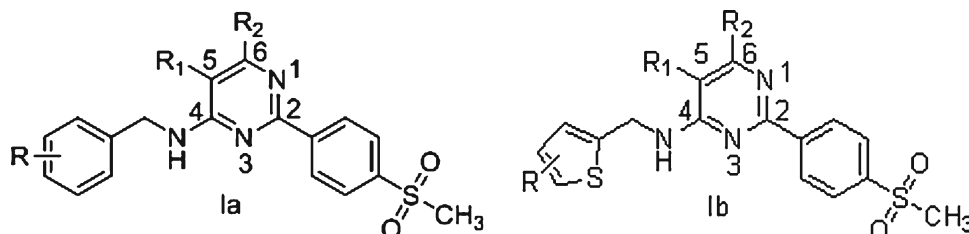
Table 4 In vitro COX-2 inhibitory activity of compounds 35–54

Compound	I	R	IC ₅₀ (μ M)	pIC ₅₀ observed	pIC ₅₀ predicted
35*	Ia	i-Pr	0.253	1.597	0.96
36	Ia	Cl	0.010	1.963	0.99
37	Ia	t-Bu	0.093	1.027	0.96
38	Ib	t-Bu	0.031	1.507	2.04
39	Ia	OMe	0.005	2.292	1.48
40	Ib	OMe	0.0004	3.398	2.65
41*	Ib	i-Pr	0.009	2.009	2.04
42	Ib	Cl	0.001	2.921	2.16
43	Ia	SEt	0.024	1.618	1.28
44	Ib	SEt	0.001	2.921	2.62
45*	Ia	SO ₂ Et	0.0907	1.042	1.47
56	Ib	NEt ₂	0.006	2.215	2.62
47	Ia	NH-i-Pr	0.273	0.563	1.53
48	Ib	NH-i-Pr	0.010	1.987	1.53
49	Ib	H	0.009	2.036	2.29
50*	Ia	OH	0.049	1.307	1.36
51	Ib	SOEt	0.037	1.425	2.43
52	Ib	OEt	0.0003	3.523	2.74
53*	Ib	OCH ₂ CH ₂ OCH ₃	0.002	2.62	2.73
54	Ib	0-Cyclopentyl	0.007	2.1215	2.85

* Compounds used for test set

represented on a grid by several different sets of fields, which provide progressively more accurate scoring of the ligand pose. The fields are computed prior to docking. The binding site is defined by a rectangular box confining the translations of the mass center of the ligand. A set of initial ligand conformations is generated through an exhaustive search of the torsional minima, and the conformers are clustered in a combinatorial fashion. Each cluster, characterized by a common conformation of the “core” and an exhaustive set of “rotamer group” conformations, is docked as a single object in the first stage. The search begins with a rough positioning and scoring phase that significantly narrows the search space and reduces the number of poses to be further considered to a few hundred. In the following stage, the selected poses are minimized on pre-computed OPLS-AA van der Waals and electrostatic grids for the receptor. In the final stage, the 5–10 lowest-energy poses obtained in this fashion

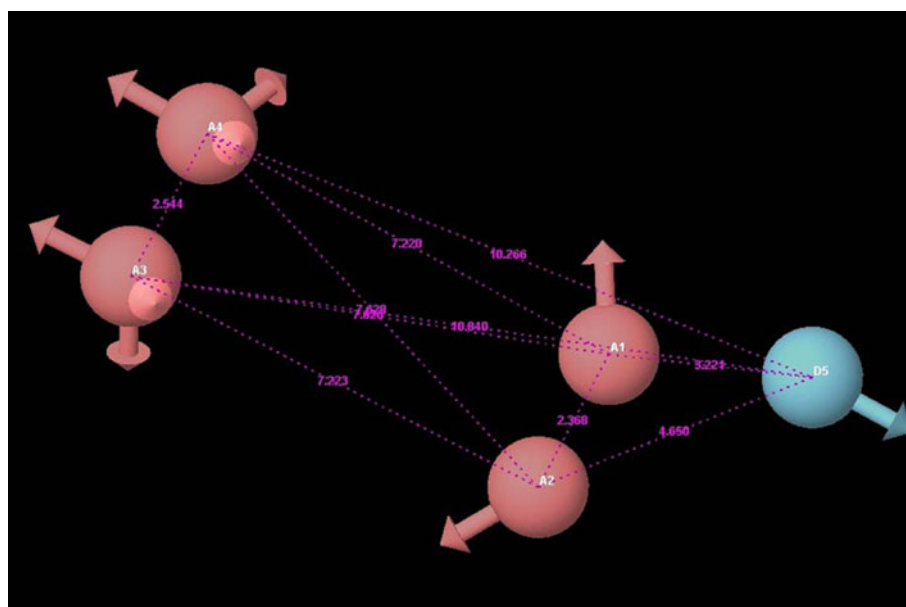
are subjected to a Monte-Carlo procedure, in which nearby torsional minima are examined, and the orientation of peripheral groups of the ligand is refined. The crystal structure of COX-2 complex with SC-558 (1CX2) was obtained from Protein Data Bank. All molecules were built within Maestro by using build, exhaustive conformational search carried out for all molecules using OPLS_2005 force field, and imposing a cutoff of allowed value of the total conformational energy compared to the lowest-energy state. Minimization cycle for conjugate gradient and steepest descent minimizations used with default value 0.05 Å for initial step size and 1.00 Å for maximum step size. In convergence criteria for the minimization, both the energy change criteria and gradient criteria, was used with default values 10⁻⁷ and 0.001 kcal/mol, respectively. A refined enzyme structure was used for grid file generation. All amino acids within 10 Å of the SC-558 were included in the grid file generation.

Table 5 In vitro COX-2 inhibitory activity of compounds 55–63


Compound	I	R	R ₂	R ₁	IC ₅₀ (μM)	pIC ₅₀ observed	pIC ₅₀ predicted
55	Ia	H	CF ₃	Me	0.018	1.745	0.99
56	Ib	H	CF ₃	Me	0.038	1.418	1.95
57*	Ia	H	CF ₃	Et	0.120	0.918	0.91
58	Ib	4-Me	Cl	H	0.044	1.353	1.00
59	Ib	4-F	CF ₃	Me	0.022	1.65	1.00
60*	Ia	4-Me	Cl	Me	0.036	1.435	0.93
61	Ia	4-F	CF ₃	Et	0.102	0.988	0.79
62	Ib	4-F	Cl	H	0.033	1.472	1.02
63*	Ia	4-F	Cl	Me	0.068	1.162	1.08

* Compounds used for test set

Figure 1 Pharmacophore hypothesis and distance between pharmacophoric sites. All distances are in Å unit



Results and discussion

Pharmacophore generation and 3D-QSAR model

A total of 22 different variant hypotheses were generated upon completion of common pharmacophore identification process. We have selected those pharmacophore models whose scores ranked in the top 1% [14]. The top model was found to be associated with the five-point hypotheses (Fig. 1), which consists of four hydrogen bond acceptor (A) and one

hydrogen bond donors (D). This is denoted as A₁A₂A₃A₄D₅. The pharmacophore hypothesis showing distance between pharmacophoric sites is depicted in Fig. 1.

The pharmacophore hypothesis yielded a 3D-QSAR model with good PLS statistics. The training set correlation is characterized by PLS factors ($r^2 = 0.642$, $SD = 0.65$, $F = 82.7$, $P = 7.617e - 12$). The test set correlation is characterized by PLS factors ($Q^2_{ext} = 0.841$, $RMSE = 0.24$, $Pearson-R = 0.91$). Results of PLS statistics of atom-based 3D-QSAR is shown in Table 6. Graph of observed versus

Table 6 Results of PLS statistics of atom-based 3D-QSAR

Training set	Test set
$r^2 = 0.642$	$Q_{\text{ext}}^2 = 0.841$,
SD = 0.65	RMSE = 0.24
$F = 82.7$, $P = 7.617e - 12$	Pearson- $R = 0.91$

SD=standard deviation of the regression, r^2 =correlation coefficient

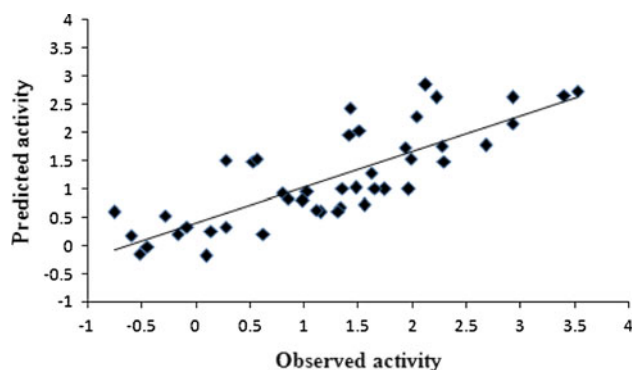
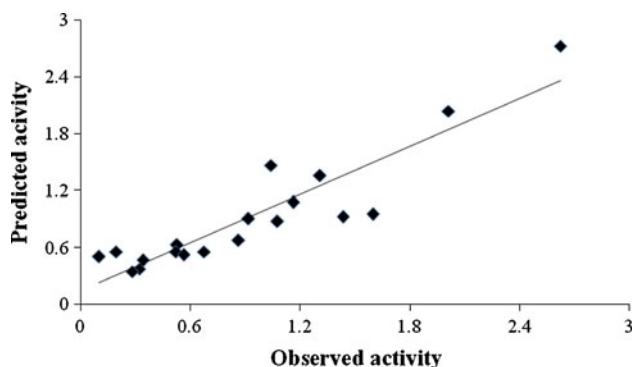
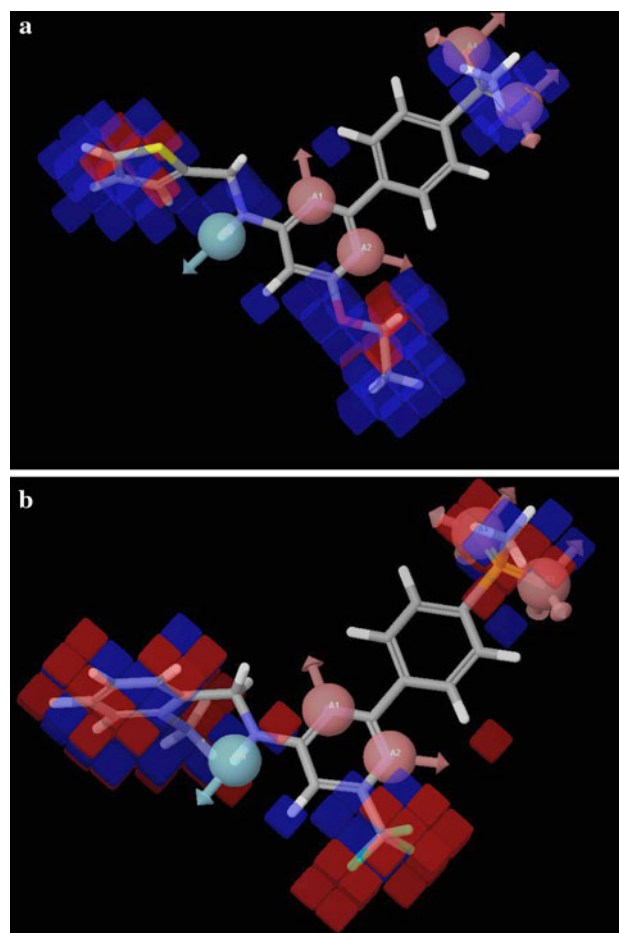
P =significance level of variance ratio, F =variance ratio

Q_{ext}^2 =for the predicted activities, RMSE=root-mean-square error

Pearson- R =correlation between the predicted and observed activity for the test set

predicted biological activity of training and test sets are shown in Figs. 2 and 3, respectively.

Additional insights into the inhibitory activity can be gained by visualizing the 3D-QSAR model in the context of one or more ligands in the series with diverse activity. A pictorial representation of the cubes generated in the present 3D-QSAR is shown in Figs. 4 and 5. In these generated cubes, the blue cubes indicate favorable features, while red cubes indicate unfavorable features for biological activity. The comparison of the most significant favorable and unfavorable interactions, which arise when the 3D-QSAR model

**Figure 2** Graph of observed versus predicted biological activity of training set**Figure 3** Graph of observed versus predicted biological activity of test set**Figure 4** Pictorial representation of the cubes generated using the QSAR model. *Blue cubes* indicate favorable regions, while *red cubes* indicate unfavorable region for the activity. Atom-based 3D QSAR model visualized in the context of the most active (a—compound 52) and least active (b—compound 26) in the training set

was applied to the most active reference ligand (compound 52) and the least active ligand (compound 26), which were shown in Fig. 4a and b, respectively.

The blue cubes around the hydrogen bond acceptor suggest that these features are important for the activity, while some unfavorable regions indicated by the reference ligand, can be justified by examining the less active molecule (compound 26). The blue cubes were observed at the position-4 near hydrogen bond donor (D_5) vector which indicated that for better activity the ring should be unsubstituted. Thus, compounds having unsubstituted ring (active compounds 39, 40, 44, 52, 54) are more active than compounds having substituted ring (inactive compounds 25, 26, 28, 29, 32) near hydrogen bond donor (D_5) vector. Moreover, Figs. 4a and 5a, b compare the most significant favorable and unfavorable features observed at the position-2 near hydrogen bond acceptor (A_3 and A_4) vector which indicated that presence of sulfonylmethyl group increases the activity. This

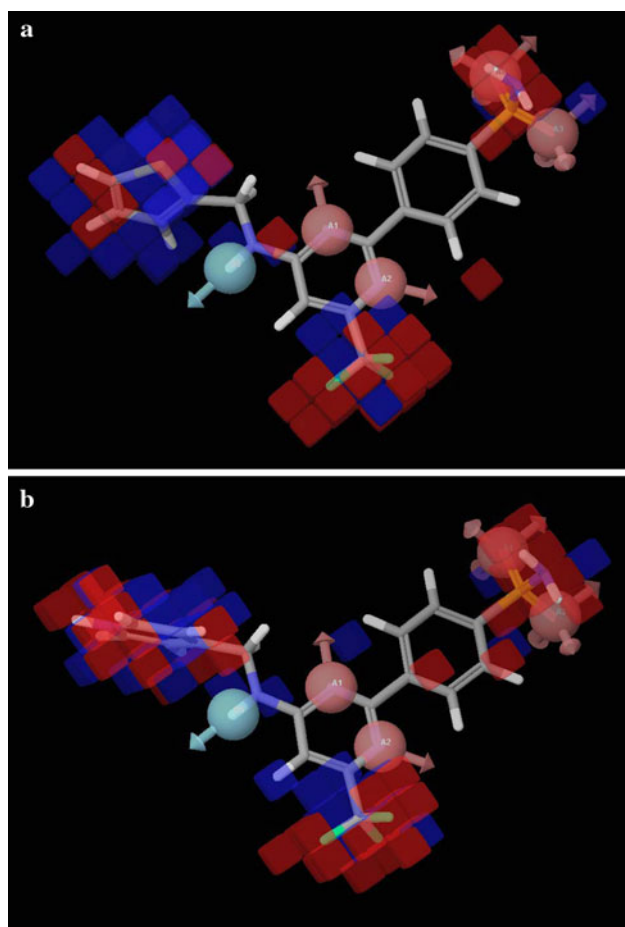


Figure 5 **a** Atom-based 3D-QSAR model visualized in the context of compound **2**. **b** Atom-based 3D-QSAR model visualized in the context of compound **5**

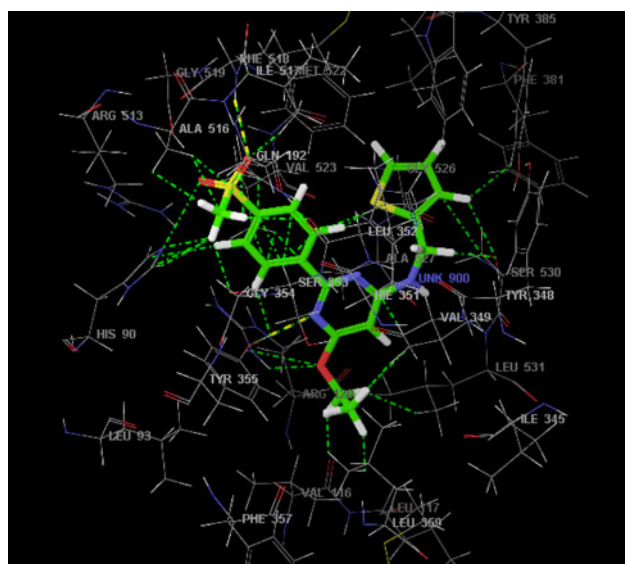


Figure 6 Docking of compound **52** in the active site of COX-2 enzyme

indicated that hydrophobic group is favorable for activity, while hydrophilic group decreases the activity. Therefore, compound having sulfonylmethyl group (active compounds **39**, **40**, **44**, **52**, **54**) are more active than compounds having sulfomoyl group (inactive compounds **2**, **5**, **7**).

Furthermore, Fig. 4a and b compares the most significant favorable and unfavorable features at position-6 near hydrogen bond acceptor (A_2) vector which indicated that electron donating groups at position-6 enhance the activity, while presence of electron-withdrawing groups decrease the activity. Therefore, compounds having electron donating substituents at position-6, such as methoxy (compound **40**) and ethoxy (compound **52**), are among the highest active compounds, while compounds having electron-withdrawing substituents (compounds **23**, **26** and **29**) are among least active compounds.

Binding mode analysis of active compounds **40** and **52** by molecular docking

Molecular docking was performed to understand the binding mode of the most active compounds **40** and **52** on COX-2 active site and to obtain information for further structure optimization, we have used extra precision glide docking (Glide XP) which docks ligands flexibly.

The docking analysis of compound **52** at COX-2 enzyme active site shows following interactions (Fig. 6): the SO_2CH_3 group interact with Arg513, Val523, Phe518, His90, and Ala516; the thiophene ring interacts with Tyr385 and Ser530; and the ethoxy group interacts with Arg120, Tyr355, and Leu531. As explained before, the electron donating groups at position-6 enhance the activity. This complies with our developed atom-based 3D-QSAR model. The docking analysis of compound **40** at COX-2 active site shows following interactions (Fig. 7): the SO_2CH_3 group interact with Arg513, Val523, Phe518, His90, and Gln192; the thiophene ring interacts with Tyr387 and Leu384; and the methoxy group interacts with Arg120 and Tyr355. Superimposition of pharmacophore hypothesis on docked ligand (compound **40**) at binding site is depicted in Fig. 8.

Conclusion

In conclusion, a highly predictive atom-based 3D-QSAR model was generated using a training set of 44 molecules which consists of five-point pharmacophore hypothesis with four hydrogen bond acceptors (A) and one hydrogen bond donor (D). The developed atom-based 3D-QSAR model can provide insights into the structural requirement of novel 2-(4-methylsulfonylphenyl)pyrimidine derivatives as selective COX-2 inhibitors. The atom-based 3D-QSAR visualization of model in the context of the structure of molecules

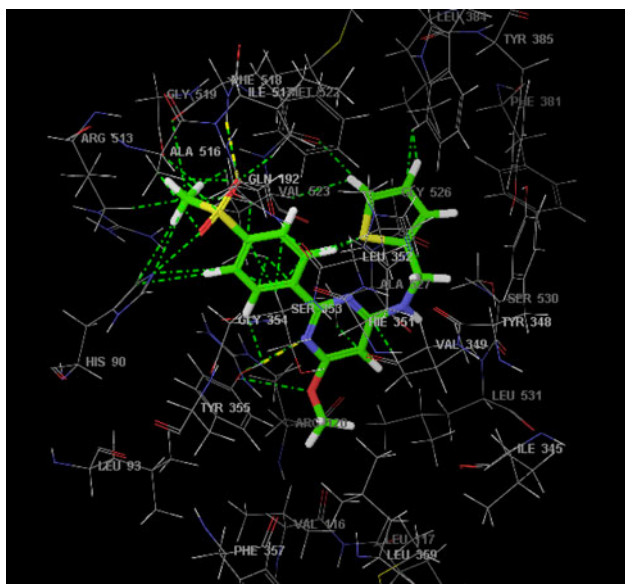


Figure 7 Docking of compound **40** in the active site of COX-2 enzyme

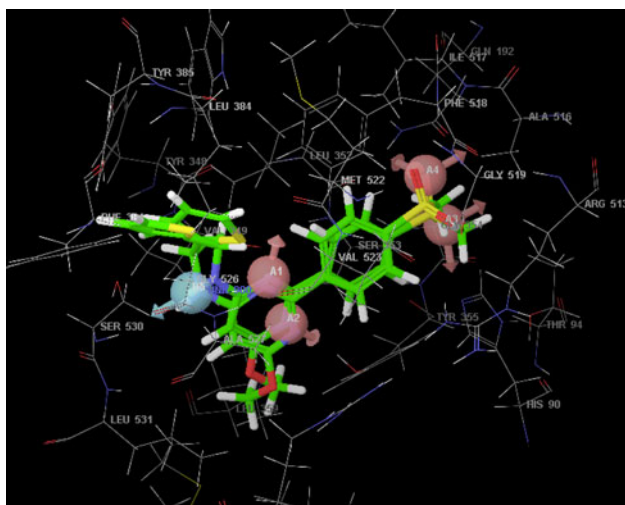


Figure 8 Superimposition of pharmacophore hypothesis on docked ligand (compound **40**) at binding site

under study provides details of the relationship between structure and activity, and thus provides information regarding structural modifications with which to design analogs with better activity prior to synthesis. Our computational studies allow for the optimization of COX-2 inhibitor as follows: the incorporation of different hydrophobic groups at position-2 as well as incorporation of different electron donating group at position-7 shall help to optimize the present series of molecules. This suggestion can be used to design new scaffolds as potent and selective COX-2 inhibitors. Furthermore, the result of our present computational study can retrieve new potential inhibitors from database using virtual screening. Thus, the results obtained from atom-based 3D-QSAR and

docking study give a hypothetical image to design new potent and highly selective COX-2 inhibitors.

The present study aimed to develop ligand-based pharmacophore hypothesis and atom-based 3D-QSAR give detailed structural insights as well as highlights important binding features of novel 2-(4-methylsulfonylphenyl)pyrimidine derivatives as COX-2 inhibitors, which can provide guidance for the rational design of novel potent COX-2 inhibitors.

Acknowledgments The authors are thankful to Dr. K. R. Mahadik, Principal, Poona College of Pharmacy, Pune.

References

- Vane JR (1994) Towards a better aspirin. *Nature* 367: 215–216. doi:10.1038/367215a0
- Penning TD, Tally JJ, Bertenshaw SR, Carter JS, Collins PW, Docter S, Graneto MJ, Lee LF, Malecha JW, Miyashiro JM, Rogers RS, Rogier DJ, Yu SS, Anderson GD, Burton EG, Cogburn JN, Gregory SA, Koboldt CM, Perkins WE, Seibert K, Veenhuizen AW, Zhang YY, Isakson PC (1997) Synthesis and biological evaluation of the 1,5-diarylpyrazole class of cyclooxygenase-2 inhibitors: identification of 4-[5-(4-methylphenyl)-3-(trifluoromethyl)-1H-pyrazol-1-yl]benzenesulfonamide (SC-58635, celecoxib). *J Med Chem* 40: 1347–1365. doi:10.1021/jm960803q
- Prasit P, Wang Z, Brideau C, Chan CC, Charleson S, Cromlish W, Ethier D, Evans JF, Ford-Hutchinson AW, Gauthier JY, Gordon R, Guay J, Gresser M, Kargman S, Kennedy B, Leblanc Y, Leger S, Mancini J, O'Neill GP, Ouellet M, Percival MD, Perrier H, Riendeau D, Rodger I, Tagari P, Therien M, Vickers P, Xu E, Wong LJ, Young RN, Zamboni R (1999) The discovery of rofecoxib, [MK 966, Vioxx, 4-(4'-methylsulfonylphenyl)-3-phenyl-2(5H)-furanone], an orally active cyclooxygenase-2-inhibitor. *Bioorg Med Chem Lett* 9: 1773–1778. doi:10.1016/S0960-894X(99)00288-7
- Talley JJ, Brown DL, Carter JS, Graneto MJ, Koboldt CM, Masferrer JL, Perkins WE, Rogers RS, Shaffer AF, Zhang YY, Zweifel BS, Seibert K (2000) 4-[5-Methyl-3-phenylisoxazol-4-yl]-benzenesulfonamide, valdecoxib: a potent and selective inhibitor of COX-2. *J Med Chem* 43: 775–777. doi:10.1021/jm990577v
- Friesen RW, Brideau C, Chan CC, Charleson S, Deschenes D, Dube D, Ethier D, Fortin R, Gauthier JY, Girard Y, Gordon R, Greig GM, Riendeau D, Savoie C, Wang Z, Wong E, Visco D, Young RN (1998) 2-Pyridinyl-3-(4-methylsulfonyl)phenylpyridines: selective and orally active cyclooxygenase-2 inhibitors. *Bioorg Med Chem Lett* 8: 2777–2782. doi:10.1016/S0960-894X(98)00499-5
- Dogne JM, Supuran CT, Pratico D (2005) Adverse cardiovascular effects of the coxibs. *J Med Chem* 48: 2251–2257. doi:10.1021/jm0402059
- Subbaramaiah K, Dannenberg AJ (2003) Cyclooxygenase 2: a molecular target for cancer prevention and treatment. *Trends Pharmacol Sci* 24: 96–102. doi:10.1016/S0165-6147(02)00043-3
- Kutcher W, Jones DA, Matsunami N, Groden J, McIntyre TM, Zimmerman GA, White RL, Prescott SM (1996) Prostaglandin H synthase 2 is expressed abnormally in human colon cancer: evidence for a transcriptional effect. *Proc Natl Acad Sci USA* 93: 4816–4820. doi:10.1073/pnas.93.10.4816
- Gasparini L, Ongini E, Wenk G (2004) Non-steroidal anti-inflammatory drugs (NSAIDs) in Alzheimer's disease: old and new mechanisms of action. *J Neurochem* 91: 521–536. doi:10.1111/j.1471-4159.2004.02743.x

10. Marriott DP, Dougall IG, Meghani P, Liu YJ, Flower DR (1999) Lead generation using pharmacophore mapping and three-dimensional database searching: application to muscarinic M(3) receptor antagonists. *J Med Chem* 42: 3210–3216. doi:[10.1021/jm980409n](https://doi.org/10.1021/jm980409n)
11. Talele TT, Kulkarni SS, Kulkarni VM (1999) Development of pharmacophore alignment models as input for comparative molecular field analysis of a diverse set of azole antifungal agents. *J Chem Inf Comput Sci* 39: 958–966. doi:[10.1021/ci990020o](https://doi.org/10.1021/ci990020o)
12. Karki RG, Kulkarni VM (2001) A feature based pharmacophore for *Candida albicans* MyristoylCoA: protein N-myristoyltransferase inhibitors. *Eur J Med Chem* 36: 147–163. doi:[10.1016/S0223-5234\(00\)01202-2](https://doi.org/10.1016/S0223-5234(00)01202-2)
13. Rarey M, Kramer B, Lengauer T, Klebe GA (1996) A fast flexible docking method using an incremental construction algorithm. *J Mol Biol* 261: 470–489. doi:[10.1006/jmbi.1996.0477](https://doi.org/10.1006/jmbi.1996.0477)
14. Phase, version 3.0, Schrödinger, LLC, New York, USA
15. Dixon SL, Smondryev AM, Knoll EH, Rao SN, Shaw DE, Friesner RA (2006) PHASE: a new engine for pharmacophore perception, 3D QSAR model development, and 3D database screening: 1. Methodology and preliminary results. *J Comput Aided Mol Des* 20: 647–671. doi:[10.1007/s10822-006-9087-6](https://doi.org/10.1007/s10822-006-9087-6)
16. Orjales A, Mosquera R, Lopez B, Oliver R, Labeaga L, Nunez MT (2008) Novel 2-(4-methylsulfonylphenyl)pyrimidine derivatives as highly potent and specific COX-2 inhibitors. *Bioorg Med Chem* 16: 2183–2199. doi:[10.1016/j.bmc.2007.11.079](https://doi.org/10.1016/j.bmc.2007.11.079)
17. Golbraikh A, Shen M, Xiao Z, Xiao Y-D, Lee K-H, Tropsha A (2003) Rational selection of training and test sets for the development of validated QSAR models. *J Comput Aided Mol Des* 17: 241–253. doi:[10.1023/A:1025386326946](https://doi.org/10.1023/A:1025386326946)
18. Maestro, version 8.5, Schrödinger, LLC, New York, USA
19. Jorgensen WL, Maxwell DS, Tirado-Rives J (1996) Development and testing of the OPLS all-atom force field on conformational energetics and properties of organic liquids. *J Am Chem Soc* 118: 11225–11236. doi:[10.1021/ja9621760](https://doi.org/10.1021/ja9621760)
20. Chang G, Guida WC, Still WC (1989) An internal-coordinate Monte Carlo method for searching conformational space. *J Am Chem Soc* 111: 4379–4386. doi:[10.1021/ja00194a035](https://doi.org/10.1021/ja00194a035)
21. Kolossvary I, Guida WC (1996) Low mode search: an efficient, automated computational method for conformational analysis—application to cyclic and acyclic alkanes and cyclic peptides. *J Am Chem Soc* 118: 5011–5019. doi:[10.1021/ja952478m](https://doi.org/10.1021/ja952478m)
22. Glide, version 5.0, Schrödinger, LLC, New York, USA
23. Friesner RA, Banks JL, Murphy RB, Halgren TA, Klicic JJ, Mainz DT, Repasky MP, Knoll EH, Shelley M, Perry JK, Shaw DE, Francis P, Shenkin PS (2004) Glide: a new approach for rapid, accurate docking and scoring. 1. Method and assessment of docking accuracy. *J Med Chem* 47: 1739–1749. doi:[10.1021/jm0306430](https://doi.org/10.1021/jm0306430)
24. Halgren TA, Murphy RB, Friesner RA, Beard HS, Frye LL, Pollard WT, Banks JL (2004) Glide: a new approach for rapid, accurate docking and scoring. 2. Enrichment factors in database screening. *J Med Chem* 47: 1750–1759. doi:[10.1021/jm030644s](https://doi.org/10.1021/jm030644s)